environments

MDPI

Article

Physicochemical Characterization of Vineyard Stump-Derived Hydrochars and Pyrochars and Preliminary Grapevine Tolerance Screening

José Manuel Díaz-Rasero [1], Teresa Sosa [2], Beatriz Ledesma [1] and Silvia Román [1,*]

[1] Department of Applied Physics, School of Industrial Engineering, University of Extremadura, 06006 Badajoz, Spain; josemanudr@unex.es (J.M.D.-R.); beatrizlc@unex.es (B.L.)
[2] Department of Plant Biology, Ecology and Earth Sciences, Faculty of Science, University of Extremadura, 06006 Badajoz, Spain; tesosa@unex.es
* Correspondence: sroman@unex.es

Abstract

This study explores a circular economy strategy for vineyard residue management through the conversion of pruning biomass into carbonaceous materials by hydrothermal carbonization (HTC) and pyrolysis (PYR), with and without iron (Fe) addition. A preliminary pot-based vegetation experiment was conducted as a screening assay to assess initial plant tolerance and exclude evident phytotoxic effects. Chlorophyll index values in grapevine leaves remained within physiological ranges across treatments and sampling dates, although no consistent treatment-related trends could be established. Overall, the results provide a physicochemical characterization of the carbonaceous materials derived from vineyard residues and demonstrate their initial compatibility with grapevine cultivation under controlled conditions. This work lays the groundwork at the material level for future, more comprehensive studies that integrate long-term soil, plant, and field assessments.

Keywords: hydrochars; pyrochars; vineyard waste; soil amendment

Check for updates

Academic Editors: Rubén Forján Castro and Elias Afif Khouri

Received: 8 December 2025
Revised: 15 January 2026
Accepted: 23 January 2026
Published: 2 February 2026

Copyright: © 2026 by the authors. Licensee MDPI, Basel, Switzerland. This article is an open access article distributed under the terms and conditions of the Creative Commons Attribution (CC BY) license.

1. Introduction

The cultivation of vineyards for wine production is a major economic activity worldwide, and the recent expansion and intensification of viticultural practices are raising increasing concerns about their impact on biodiversity. Systematic reviews and meta-analyses indicate that organic viticulture and aboveground vegetation management (e.g., cover crops) enhance biodiversity and ecosystem services such as soil fertility, pest control, and carbon sequestration [1]. Maintaining inter-row vegetation is particularly beneficial, with no significant trade-off between grape yield and biodiversity [2]. Nevertheless, two fundamental challenges persist in vineyard systems: the impacts of climate change, including increasing drought frequency, and the progressive loss of soil nutrients and productivity under intensive management. Soil erosion caused by intense rainfall in Mediterranean vineyards leads to nutrient loss (as nitrogen, phosphorus, potassium, and organic carbon), degradation of soil structure, and reduced organic matter, all of which directly affect grape productivity and quality [3]. Studies in southern Italy confirm a negative correlation between soil erosion and vine productivity [4]. These effects are further exacerbated by intensive practices and excessive agrochemical use, which contribute to long-term soil degradation. In parallel, water scarcity associated with climate change represents an additional constraint on vineyard sustainability. In this context, alternatives are needed to

sustain vineyard productivity and grape quality while addressing water and nutrient limitations. One potential strategy involves the valorization of vineyard residues to produce carbon-based materials with properties that may be relevant for agricultural soils. Within the framework of the circular economy, hydrothermal carbonization (HTC) offers a promising approach due to its low cost and ability to process high-moisture wastes. HTC generates both solid hydrochar (HC) and process water (PW), each with versatile applications [5]. Hydrochars are increasingly investigated in soil-related contexts, although their effects remain variable and strongly context-dependent, while pyrochars (PIRs) have a longer history of study, particularly in relation to carbon sequestration [6]. Unlike pyrolysis (PYR), HTC involves lower direct CO_2 emissions, typically reported in the range of 5–10% of the initial biomass carbon, which has increased interest in HTC within short-term decarbonization strategies.

The literature presents mixed results regarding the effectiveness of HCs in soils. Reported effects vary widely depending on the feedstock, hydrothermal carbonization conditions [7], crop type, and soil properties. For example, reductions in soil mineral nitrogen of 20–50% and increases in microbial biomass of up to 30% have been observed following HC application [8]. In some cases, HCs increase soil pH by 0.2–1.0 units and enhance biomass production in specific crops, whereas in others they may reduce nitrogen uptake [9]. Certain amino-functionalized HCs have been shown to decrease available heavy metals by 15–40% and improve plant growth under contaminated conditions [10]. Improvements in water retention (5–15%), reductions in bulk density, and increases in microbial abundance suggest that HCs may influence soil processes related to organic carbon stabilization [11,12]. However, these effects are not universal and should not be assumed without site-specific validation. Positive effects on plant growth and water-use efficiency under heat stress have also been documented in selected systems [13]. Recent studies have examined vineyard residues processed by HTC or PYR and their impact on biodiversity and ecosystem services. Grape pomace can be efficiently converted into hydrochar, with yield and quality depending on HTC conditions [14], although liquid fractions show lower biogas yields due to recalcitrant nitrogen compounds [15]. To date, no studies have specifically investigated the hydrothermal carbonization of vineyard stumps (VSs), as most existing research has focused on grape pulp [16], pruning residues for energy applications [17], or techno-economic assessments of HTC plants using vine shoots [18]. Pyrochars provide long-term benefits to vineyard soils by improving their physical, chemical, and biological fertility. They can also reduce soil erosion by enhancing aggregate stability, increasing infiltration through improved porosity, and modifying surface roughness, which slows overland flow. Field studies up to 10 years report increases in soil organic carbon, higher pH, reduced bulk density, and improved water retention, mitigating drought stress [19,20]. Other studies highlight enhanced cation exchange and microbial community shifts, with increased beneficial fungi and reduced pathogens [21,22]. Productivity outcomes are variable, with some reporting yield improvements but limited effects on wine quality. In this variability, in the case of vineyards, biochar amendment at rates up to 2.55 L m^{-2} resulted in a non-significant improvement in grape yield per plant. The high variability in response was largely due to the adverse climatic conditions typical of the Csa region's Mediterranean climate, which masked the observed positive trends. Such variability is common in biochar studies, as the agronomic response depends heavily on the application rate, soil characteristics, and the physicochemical properties of the biochar used. Conversely, under different climatic conditions and soil types, such as those found at two Oregon sites (Willamette Valley and Rogue Valley), biochar applied at rates up to 35 t ha^{-1} produced distinct results, highlighting the strong influence of climate–soil–biochar interactions on vineyard yield [23–25]. PIRs from vine shoots, cuttings, or canes also improve water retention and

nutrient availability [26], though performance depends on pyrolysis temperature and raw material [27,28].

To date, no previous study has evaluated vineyard vines as a raw material for hydrothermal carbonization, nor has it assessed the properties of the resulting carbonaceous materials for potential soil applications. Against this background, the present study focuses on the production and physicochemical characterization of hydrochars and pyrochars derived from vineyard stumps (VSs) obtained from an agricultural cooperative in central-southern Spain. As a novel aspect, vineyard stumps were subjected to hydrothermal carbonization, a feedstock–process combination that has not been previously reported for viticultural systems. All prepared carbon materials were subsequently evaluated in a preliminary pot-based experiment designed as a tolerance screening, aimed at identifying potential phytotoxic or strongly negative effects on grapevine plants. FTIR analysis was employed to characterize the surface functional features of the carbon materials, providing indirect insight into properties that may be relevant for soil interactions, while chlorophyll index measurements were used as a non-destructive indicator of plant physiological status. In addition to comparing HCs and PIRs derived from vineyard stumps, this study also explores iron (Fe) incorporation via ferric chloride ($FeCl_3$) as a surface modification strategy. The rationale for Fe-enrichment is based on its ability to introduce Fe-O bonds and modify surface chemistry, which could broaden the functional properties of the materials and potentially lead to improvements in soil fertility. Such modification may broaden the range of potential applications of vineyard-derived carbonaceous materials, which warrant further investigation in future soil-based and field-scale studies. Table 1 below summarizes the main previous results related to HTC and pyrolysis related to grapevine.

Table 1. Summary of key previous results from HTC and pyrolysis in grapevines.

Topic/Study	Main Findings	Ref.
Effect of organic viticulture and vegetation cover	Increase biodiversity and ecosystem services (soil fertility, pest control, carbon sequestration).	[1,2]
HTC: products and applications	HTC produces solid hydrochar (HC) and process water (PW); viable for wet residues and circular economy uses.	[5]
Contrasting roles of HC and PIR	HC improves CEC and nutrient retention; PIR is more stable and favors carbon sequestration.	[6]
Variable HC outcomes in soils	Effects depend on feedstock and HTC conditions; HC can act as herbicide or fertilizer; results are heterogeneous	[7–10]
HC and soil properties	HC improves water retention, reduces bulk density, increases microbial biomass and carbon sequestration.	[11,12]
Plant responses under heat stress	HC showed positive effects on growth and water use efficiency under heat.	[13]
Conversion of vineyard residues by HTC	Grape pomace convertible to HC; yield and quality depend on HTC conditions.	[14,15]
Gap in vineyard stumps (VSs)	No specific studies applying VSs as HTC amendments identify as a knowledge gap.	[16–18]
Long-term benefits of PIR	Increases in soil organic C, pH, water retention and reduced bulk density in study up to 10 years.	[19,20]
Biological and productivity effects of PIR	Changes in CEC and microbial communities; effects on yield and wine quality are variable.	[21–25]
PIR and water/nutrient availability	PIR improves water retention and nutrient availability; performance depends on pyrolysis temperature and feedstock	[26–28]

2. Materials and Methods

2.1. Materials

Vineyard stumps (VSs), sourced from the Yuntero Cooperative, located in Manzanares, Castilla-La Mancha region (Spain), was used as feedstock in this study. This raw material was supplied in big pieces and needed mechanical conditioning: VS pieces were initially cut with a chainsaw then the sawdust generated during the cutting process was grinded. The remaining stump material was shredded using a GARLAND Chipper 790 Qg-V19. The shredded material was then thoroughly mixed with the sawdust to obtain a uniform appearance, producing a homogeneous size product. After shredding and mixing, the material was sieved to obtain a final particle size distribution between 1 and 4 mm (sieve, CISA 200/50, Norma ISO-3310.1) [29], which was selected to ensure homogeneous reaction kinetics during HTC and to reduce mass-transfer limitations.

2.2. Experimental Reactions

2.2.1. HTC Reactions

HTC reactions were carried out using a Parr 4848 reactor (Parr Instrument Company, Moline, IL, USA) with a total capacity of 1.2 L. The reaction mixture consisted of 720 g of water and 210 g of biomass (wet basis, without prior drying), corresponding to a solid-to-liquid ratio of 0.22. The components were thoroughly mixed and introduced into the reactor.

Heating to the target temperature was conducted over 90 min, including the heating ramp, and once the maximum temperature of 220 °C was reached, it was maintained for a residence time of 18.5 h. After completion of the reaction, the reactor was allowed to cool naturally to room temperature before opening. The resulting slurry was filtered, and the solid fraction was dried in an oven at 105 °C for 12 h. The obtained hydrochar (HC) was collected and stored in airtight containers. Multiple HTC runs were conducted to obtain sufficient material for subsequent analyses and preliminary plant assays. HTC reactions were also performed to enrich the HC obtained in Fe. To this end, the HTC reactions were carried out under the same temperature and time conditions but replacing the mentioned amount of water with a 0.25 M $FeCl_3 \cdot 6H_2O$ solution, as described in [30]. This solution was mixed directly with the biomass in the reactor before HTC process.

2.2.2. Pyrolysis Reactions

Pyrolysis was carried out in a stainless-steel tubular reactor at 600 °C for 1 h under a continuous N_2 flow of 100 mL/min to ensure an inert atmosphere. The starting material was 150 g of VS. After completion of the reaction, the reactor was allowed to cool in air while maintaining the N_2 flow to prevent combustion. The resulting PIR was then collected and stored for later use.

This reaction also produced Fe-enriched PIRs, following the procedure described in [31]. For this process, 10 g of dried and sieved biomass were added to 150 mL of a 0.25 M $FeCl_3 \cdot 6H_2O$ solution in a glass flask. The flask was capped and placed in a bath sonicator (40 kHz, 150 W) for 1 h 15 min at room temperature to enhance the interaction between the biomass and Fe^{3+} ions. Subsequently, the suspension was kept under magnetic stirring at 25 °C for 24 h, protected from light with aluminum foil to avoid Fe^{3+} photoreduction. After incubation, the solid was separated by drip filtration, washed with deionized water to remove unbound Fe, and dried in an oven at 105 °C for 48 h.

2.3. Characterization of Hydrochars, Pyrochars and Raw Material

The elemental composition (C, H, N, and S) of the HCs, PIRs and raw material were determined using a CHNS analyzer (LECO CHNS-932, LECO Corporation, St. Joseph,

MI, USA). The O content was estimated as the difference between the sum of the above and the ash content at 100%. The fuel value of these materials was characterized by the higher heating value (HHV) measured in a calorimetric bomb (PARR), following the norm CEN/TS 14918. Lower heating value (LHV) was calculated by Equation (1):

$$\mathrm{LHV} = \mathrm{HHV} - 2.442 \cdot 9\mathrm{H}, \quad (1)$$

where HHV is expressed in MJ kg^{-1} and H correspond to the hydrogen content (% dry basis) of the sample and 2.442 (MJ kg^{-1}) is the latent heat of vaporization of water associated with hydrogen combustion. The lower heating value (LHV) is expressed on a dry basis. Ion chromatography (IC) was applied to raw vineyard stump material to quantify the chloride content before thermochemical treatment, with the aim of evaluating the suitability of the raw material for subsequent conversion processes. The methodology consists of extracting the sample in an aqueous solution, filtering it, and then injecting it into an ion-exchange column where the anions present, including chlorides, are separated based on their affinity for the chromatographic resin. A conductivity detector measures chloride concentration, allowing its quantification with high sensitivity in the ppm (mg/kg) range. This technique is precise and effective for environmental studies and material characterization.

The proximate analysis (moisture, volatile matter, ash, and fixed carbon) was performed on the raw samples, using an STA 449 F3 Jupiter (Netzsch, Berlin, Germany) thermobalance in an oxidizing atmosphere (20% oxygen and 80% argon with a flow rate of 100 mL/min) using a ramp from 20 °C/min up to 700 °C.

For hydrocahrs, pyrochars, HC_Fe and PIR_Fe samples, FTIR and SEM analysis were made too. FTIR spectra were recorded with a Perkin Elmer model Paragon 1000PC spectrophotometer with a resolution of 4 cm^{-1} and 100 scans, equipped with a diamond crystal ATR accessory in attenuated total reflectance (ATR) mode.

The surface morphology of the samples was analyzed by scanning electron micrography (SEM, Hitachi, S-3600 N, Krefeld, Germany) observation. The SEM samples were prepared by depositing about 50 mg of sample on an aluminum stud covered with conductive adhesive carbon tapes, and then coating with Rd–Pd for 1 min to prevent charging during observations. Imaging was performed in the high vacuum mode at an accelerating voltage of 20 kV, using secondary electrons.

The ash content of all samples was measured directly after dry oxidation at 550 °C according to the DIN EN 14775:2010-04 standard.

2.4. Analyses for Plant Evolution in Field Tests

2.4.1. Chlorophyll Index

Chlorophyll index in the leaves of each plant was measured to gather information about the nutrient status and stress levels of the plants. Using a chlorophyll meter (MC-100, Apogee Instruments, Logan, UT, USA), measurements were taken three times on the following dates: 26-June 30-July and 10-Septempter. For each plant, three fully expanded leaves of similar size and developmental stage were selected from the middle part of the shoot, as recommended for consistency in physiological studies [32]. Chlorophyll index was recorded directly on each leaf, and the average of the three measurements was calculated to obtain a representative value per plant.

Subsequently, the average chlorophyll index was calculated for all plants with each type of carbons. All data are expressed in Relative Units (r.u.). No conversion to absolute chlorophyll concentration was performed.

2.4.2. Efficacy Trials on the Soil Application of HCs and PIRs

The plant trial was designed as a preliminary tolerance and non-phytotoxicity screening prior to field-scale experiments, rather than as an evaluation of agronomic performance.

Pot-based systems were selected to allow controlled amendment concentrations and direct observation of early plant responses. However, these systems have known limitations, such as restricted root development, reduced soil aeration, limited water retention, and increased heat stress, especially under high summer temperatures. These limitations can increase plant mortality regardless of treatment effects and are recognized as an inherent disadvantage in early-stage analytical experiments.

This trial involved planting 96 vines from the Yuntero Cooperative, with the addition of prepared carbonaceous materials at 1% and 3% (*v*/*v*). The experiment was designed to evaluate HCs produced at 220 °C, pyrochars produced at 600 °C, and their iron Fe-enriched variants.

Figure 1 illustrates the spatial arrangement of the 96 pots according to treatment type and concentration. The grid-based layout was applied to ensure systematic distribution of treatments, with three replicates per treatment, although the design was not intended for inferential statistical comparison among treatments.

	93	91	1	11	21	31	41	
Control	83	81	42	2	12	22	32	
41D	73	71	33	43	3	13	23	11D
41C	63	61	24	34	44	4	14	11C
41B	53	51	15	25	35	45	5	11B
41A	92	90	6	16	26	36	46	11A
31D	82	80	47	7	17	27	37	21D
31C	72	70	38	48	8	18	28	21C
31B	62	60	29	39	49	9	19	21B
31A	52	50´	20	30	40	50	10	21A

Control	
HC (1%)	HC (3%)
PIR (1%)	PIR (3%)
HC_Fe (1%)	HC_Fe (3%)
PIR_Fe (1%)	PIR_Fe (3%)

Figure 1. Spatial distribution of the 96 experimental pots according to treatment type and concentration. The layout follows a grid-based design inspired by Roman *centuriation*. Color coding indicates the type and percentage of carbon applied: HC (1% and 3%), PIR (1% and 3%), PIR_Fe (1% and 3%), HC_Fe (1% and 3%) and control. Labels correspond to pot identifiers used throughout the experiment.

Each pot was filled with soil collected from the cooperative's land. The experiment was conducted at the School of Agricultural Engineering in Badajoz, approximately 300 km from the sampling site. Both locations share comparable Mediterranean climatic conditions (Csa climate according to Köppen–Geiger classification).

Planting was initiated on 29 May 2024, in accordance with the established experimental design. A total of 52 sprouted plants were placed into pots and watered to field capacity, without the addition of PIRs or HC at this initial stage. The pots were then placed in the greenhouse, while the remaining plants were stored in a growth chamber for planting in the following days.

On 30 May 2024, a preliminary inspection confirmed that all pots contained sprouted plants. This early sprout was later determined not to interfere with the experimental outcomes.

On 12 June 2024, PIRs and HC were incorporated at a concentration of 1% into the 52 pots, followed by irrigation with 300 mL of water per pot. The pots were returned to the greenhouse and appropriately labeled. On 17 June 2024, an additional application of 3% HC was made to the pots labeled 11A, 11B, 11C, and 11D.

A second labeling phase took place on 20 June 2024, during which the pots were relocated outdoors. The remaining 44 pots received their respective carbon treatments and were irrigated with 300 mL of water. All the pots were watered weekly during the summer season.

Figure 2 shows the experimental pots after relocation outdoors, with visible labels and treatment assignments. The dimensions of the pots are: diameter 16.5 cm, height 41 cm, height of soil content: 34.5 cm. All the pots have drainage holes.



Figure 2. Example of experimental pots arranged outdoors following treatment application and labeling.

Despite manual watering throughout the summer, with applications of approximately 300 mL per pot, two to three times per week, depending on observed field capacity, plant survival was compromised by extreme environmental conditions. During the summer period, maximum temperatures reached up to 45 °C, along with episodes of very high solar radiation (UV index ≈ 10) and heat waves lasting up to a week. These factors were intensified by the high thermal absorption of the black pots used. Furthermore, in January 2025, minimum temperatures as low as −3 °C were recorded, which may have further affected plant development. These conditions, exacerbated by the high thermal absorption of black pots, are recognized as significant abiotic stress factors and are discussed as limitations of the experimental system, reinforcing the screening nature of the trial. Due to the exploratory nature of the vegetation experiment and the limited number of replicates per treatment, no inferential statistical analyses were applied.

3. Results and Discussion

3.1. Raw Materials

Table 2 presents the physicochemical properties of the raw material (VS) used in the experiment (all determined in dry basis). These parameters are relevant for contextualizing behavior during carbonization and its potential suitability for subsequent soil-related applications.

Table 2. Characterization of vine stumps (VSs).

Proximate Analysis	**%**
Volatile matter	81.27
Fixed carbon	17.25
Ash	1.48
Elemental analysis	**%**
C	45.10
H	6.05
N	0.31
S	0.03
O [1]	47.03
HHV	MJ/kg
0% moisture	19.32
Moisture received	17.57
LHV	MJ/kg
0% moisture	17.99
Moisture received	16.37

[1] Calculated by difference.

The VS has a moderate moisture content (9.06%), which reduces the need for thermal pretreatment prior to carbonization. Its high volatile organic content (81.27%) can influence the porous structure of different PIRs or HCs, as during pyrolysis and HTC, molecules susceptible to elimination (mainly hemicellulose and cellulose) can open cavities in the material's structure. This porosity is related to its water adsorption and retention capacity during subsequent application. The fixed carbon content (17.25%), a typical value for lignocellulosic biomasses such as wood or fruit pits, suggests greater stability of the carbonized material, which is desirable for its persistence in the soil. Furthermore, its low ash content (1.48%) indicates a lower presence of mineral impurities, which can improve the quality of biochar for agricultural soils. For all samples in the following Table 2, the average values are shown in the table, with the deviation being less than 5% in all cases, as three repetitions were performed for the samples.

In terms of elemental composition, VS has a carbon content of 45.10%, characteristic of lignocellulosic biomasses, which can favor the chemical stability of biochar in the soil. Its hydrogen (6.05%) and oxygen (47.03%) content can influence the material's reactivity in carbonization processes. Furthermore, its low nitrogen content (0.31%) minimizes the formation of volatile nitrogen compounds during the thermochemical process, reducing pollutant emissions.

Overall, as shown in Table 2 the proximate and elemental analyses are typical of lignocellulosic biomasses, very similar to other woods. Thus, the carbon content and the volatile content indicate a high proportion of volatile carbon and high calorific value. The low ash content also suggests that this biomass generates little solid waste when burned, which is beneficial from both an environmental and equipment maintenance perspective. These similarities support the suitability of VS as a representative woody residue for comparative carbonization studies. Woods from pruned oak, almond, and walnut trees, previously studied by the research group, have shown similar results.

The calorific value of biomass reflects its energy potential; however, in the present work, the primary objective was not energy recovery but transformation into hydrochars and pyrochars for material characterization and preliminary plant compatibility assessment. From this perspective, the VS feedstock provides favorable conditions for obtaining carbon materials with relatively high carbon content and low ash fractions. Regarding chloride

content, the VS showed a higher concentration (249.90 mg/kg) compared to other residual material from the grape, such as the skins (from the crushing of the grape pulp). This material has a value of around 130 mg/kg. This difference may be due to the composition and structure of each material, since the VS, being more lignocellulosic than the grape, may have accumulated more mineral salts during the growth of the vine. Furthermore, the prolonged contact with the soil could have favored chloride retention compared to the skins, which come from the more superficial part of the fruit. The determination of chloride content is important because chlorine promotes the formation of corrosive compounds and deposits during thermochemical conversion, which can compromise equipment durability and process stability. It is also linked to regulated emissions, so quantifying chloride helps assess the suitability of the material as a biofuel beyond its energy potential.

3.2. Analysis of PIRs and HCs

The PIRs and HCs have been characterized according to their elemental analysis, HHV, and solid yield (Table 3). These results provide a comparative description of the materials obtained under different processing conditions and with or without iron enrichment. Regarding the HCs, a decrease in HHV and an increase in solid yield are notable for the iron-enriched HC compared to the iron-free HC. This may be because $FeCl_3$ creates a highly acidic environment that promotes the hydrolysis and solubilization of the biomass's organic components, reducing the carbonaceous fraction. However, this also causes some of the iron to precipitate and be retained in the hydrochar as oxides and hydroxides [33]. This iron incorporation increases the final mass of the solid, thus increasing the yield calculated as final mass divided by initial mass. Nevertheless, since the enriched hydrochar contains more ash and less organic carbon, its energy density decreases [34], the calorific value is reduced because the mineral fraction does not contribute energy to combustion and dilutes the available carbon content, (Table 3). For all samples in the following Table 3, the average values are shown in the table, with the deviation being less than 5% in all cases, as three repetitions were performed for each HC/PIR sample.

Table 3. Characterization of HCs and PIRs.

Sample	Solid Yield (%)	C (%)	N (%)	H (%)	S (%)	O [1] (%)	Ash (%)	HHV (MJ/kg)
PIR	27.13	68.64	0.67	3.32	0.10	18.32	8.95	30.11
HC	58.81	64.00	0.77	6.25	0.21	25.26	3.51	30.62
PIR_Fe	30.02	65.87	0.63	3.47	0.12	16.27	13.64	25.92
HC_Fe	62.90	54.30	0.50	5.27	0.18	36.21	3.54	21.06

[1] calculated by difference.

Something similar occurs with PIR samples. During pyrolysis, high temperatures in the absence of oxygen cause the thermal decomposition of the organic components of the biomass. If $FeCl_3$ is present in the mixture, the iron acts as a catalyst, promoting the breaking of bonds in cellulose, hemicellulose, and lignin, and accelerating the formation of volatile products and gases. This means that some of the carbon that would normally remain in the biochar is transferred to the gaseous or liquid phase, reducing the organic fraction of the solid. However, at the same time, iron is incorporated into the biochar in the form of oxides or inorganic compounds, increasing the final mass of the solid and making the apparent yield higher. The result is a biochar with more ashes and less available carbon, which explains the decrease in calorific value [35].

Another aspect to analyze is the apparent increase in nitrogen content in the HC and PIR samples compared to the initial biomass. This increase does not imply the formation

of new nitrogen during carbonization but should be interpreted as a concentration effect resulting from the loss of volatile mass during the HTC or pyrolysis processes. The nitrogen present in the biomass, mainly in the form of proteins, can be transformed during HTC by hydrolysis at relatively low temperatures (≈120 °C) [36], generating amino acids that can subsequently undergo decarboxylation, deamination, or participate in Maillard reactions, producing amines, ammonia, organic acids, or N-cyclic compounds. However, since this study did not provide data on the protein content of the original biomass, it is not possible to accurately determine which pathways dominate in N retention in the final solid. Even so, regardless of the initial protein content, the resulting biochar typically retains a fraction of the original nitrogen, possibly incorporated through Maillard reactions, as described in previous studies [37].

Regarding the surface morphology (Figure 3) of the different samples, the greatest differences are observed between HC and HC_Fe. The presence of iron during hydrothermal carbonization has a clear influence on the surface morphology of the resulting hydrochars. Without iron, the hydrochar typically exhibits a compact and relatively homogeneous structure, characterized by smooth or only mildly textured surfaces and limited visible porosity. The carbon matrix tends to form dense agglomerates with few open cavities, reflecting the milder progression of dehydration, depolymerization, and structural rearrangement when no catalytic species are present. As a result, the material displays a more closed morphology with a lower degree of surface development. In contrast, the incorporation of iron leads to pronounced modifications in the microstructure. Iron acts as a catalytic agent, promoting more extensive bond cleavage, dehydration, and condensation reactions during the hydrothermal process. Consequently, the hydrochars produced in the presence of iron show markedly rougher and more heterogeneous surfaces, with the formation of pores, fissures, and irregular cavities distributed throughout the matrix. This enhanced textural development indicates a deeper structural transformation of the precursor material. The presence of secondary hydrochar can be seen in both HC samples, with the shape of spheres on the surface of both samples.

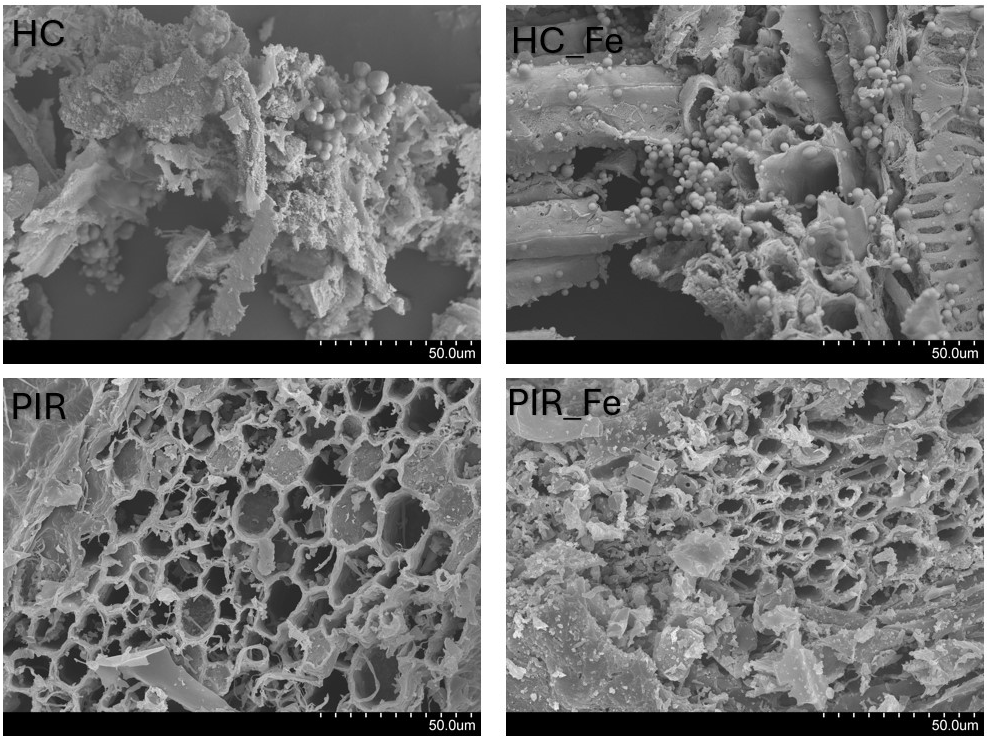


Figure 3. SEM of HC, HC_Fe, PIR and PIR_Fe samples.

In pyrolysis, the thermal severity of the process already produces a highly devolatilized and porous carbon matrix, which means that the material naturally develops a rough, fractured surface regardless of whether iron is present. Because the structural breakdown, aromatization, and pore formation are largely driven by high temperature, the additional catalytic effect of iron has a comparatively smaller impact on the final morphology. As a result, both PIR and PIR_Fe tend to exhibit similar surface textures in SEM, with only subtle differences such as slightly enhanced porosity or localized iron-rich domains in the Fe-treated samples. The dominant influence of temperature during pyrolysis therefore reduces the visual contrast between samples produced with and without iron (Figure 3).

Thus, the differences between HCs and PIRs can be attributed to several factors. Thus, HTC involves a series of temperature and pressure driven reactions, including hydrolysis, dehydration, decarboxylation, and condensation, which progressively transform wet biomass into a carbon rich solid. As a result of these reaction pathways, HCs typically exhibit higher oxygen content, lower aromaticity, and greater surface functionality than PIRs produced through dry thermal decomposition. These compositional differences suggest potentially distinct behaviors in soil environments. From an environmental perspective, HTC offers advantages such as the ability to process wet feedstocks without prior drying and the potential for lower emissions, although HCs generally show lower long term carbon persistence compared to PIRs.

3.3. Analysis of Chlorophyll Index

The effect of the different treatments on the chlorophyll index of each plant was evaluated over three measurement dates: 26 June 2024, 3 July 2024, and 10 September 2024. The average chlorophyll index recorded for each treatment and date is summarized in Table 4. Overall, values ranged between 22 and 31 (r.u.) which are within the physiological range typically reported for grapevine [38]. Across all pots, an increase in chlorophyll index was observed from June to July, followed by a decline in September. This seasonal pattern has been described in grapevine and other woody species and reflects leaf maturation followed by the onset of senescence and summer stress conditions [39]. This trend was observed across treatments, including controls, indicating a dominant influence of seasonal and environmental factors. Some Fe-enriched treatments (e.g., 3%PIR_Fe) showed comparatively higher chlorophyll values at certain time points, while others (e.g., 3% HC_Fe) exhibited lower values at the final sampling. However, no consistent or systematic pattern associated with a specific treatment or concentration was identified. Given the preliminary nature of the trial and the absence of inferential statistical analysis, these observations should be interpreted as descriptive trends rather than treatment effects.

Table 4. Chlorophyll index (r.u.) measured in vine leaves at different sampling dates under the different treatments.

	Control	1%HC	1%PIR	1%HC_Fe	1%PIR_Fe	3%HC	3%PIR	3%HC_Fe	3%PIR_Fe
26 June 2024	27.2	28.6	28.1	28.3	29.1	29.3	-	-	-
3 July 2024	30.0	30.6	29.7	30.5	29.0	25.0	24.0	29.6	31.4
10 September 2024	24.0	24.3	22.5	25.7	23.3	-	31.4	17.3	26.1
Average	27.1	27.9	26.8	28.2	27.1	27.2	27.7	23.4	28.7

Average values presented in Table 4 correspond to deviations below 4%, based on repeated measurements. The chlorophyll index data was used solely as a non-destructive indicator of plant physiological status to screen for evident phytotoxic responses.

3.4. HTC Reaction Pressure

During the HTC reaction, differences in the pressure generated during the process were observed. Thus, in HTC reactions using iron-enriched biomass, significantly lower pressures were obtained than in reactions with the same biomass and under the same conditions, but without iron enrichment (23.8–35.3 bar respectively). This pressure reduction upon addition of $FeCl_3$ during HTC is primarily due to three interrelated effects: lower net generation of gaseous moles due to the diversion of matter to the solid phase (more hydrochar formation), capture/transformation of volatile species (especially sulfur compounds), and changes in the chemistry of the medium (pH and redox) that alter decomposition pathways.

Chemically, Fe^{3+} acts as an acid/oxidizing catalyst that promotes dehydration, condensation, and aromatization reactions in the lignocellulosic matrix, increasing carbon retention in the hydrochar and reducing the volatile fraction susceptible to gas formation during the HTC [33].

Additionally, Fe can precipitate or form complexes with sulphur species and soluble fractions of the biomass, causing coagulation and solid-phase sequestration that decreases the contribution of compounds such as H_2S to the total pressure. $FeCl_3$ hydrolysis also acidifies the medium, shifting equilibria toward less volatile products and promoting greater stabilization in the form of solids or non-gaseous liquids [40].

To quantitatively attribute the drop of the pressure, it is useful to measure the gas composition (GC for CO_2, H_2, CH_4, H_2S, CO), the yield and elemental characterization of the hydrochar, sulphur and Fe–S phase analysis in the solids (XRD/SEM EDX), and pH/Fe dissolved in the liquor. Tests with different FeCl doses and time-based replicates allow for the dose-effect dependence to be traced and mass balances to be established that explain the extent to which solid sequestration or volatile reduction is responsible for the observed pressure decrease [41]. However, this would exceed the objectives of this work, so further studies would be necessary in this area and with other biomasses.

3.5. FTIR Analysis

The FTIR spectra of the original samples and their evolution over time were analyzed in open-air conditions (19 July 2024, 29 November 2024 and 27 February 2025) to identify signs of degradation and changes in surface functional groups.

The study established key differences in the chemical composition and stability of the materials: HC_original; PIR_original (original pyrochar); HC_Fe_original (Fe-doped HC); PIR_Fe_original (Fe-doped PIR).

The spectra obtained were compared with the same samples analyzed after months of exposure under ambient conditions. The nomenclature use for each sample is: HC/PIR _day–month–year.

First, the differences between HC and PIR were analyzed. The HC samples (Figure 4) present a higher content of surface oxygenated groups compared to the PIR, reflected in more intense bands in the following regions:

3200–3400 cm^{-1} (O-H): Greater intensity in HC, indicating the presence of hydroxyl groups. 1700 cm^{-1} (C=O): Notable in HC, attributed to carbonyls of carboxylic acids and esters. 1600–1500 cm^{-1} (aromatic C=C/COO^-): More pronounced in PIR, suggesting a more graphitic and less functionalized structure [42]. 1200–1000 cm^{-1} (C-O): More prominent in HC, reflecting the presence of alcohols and ethers.

The PIR samples (Figure 5), in contrast, show lower intensity in these bands and a more pronounced signal at 1580 cm^{-1}, indicative of more condensed aromatic structures. This confirms that pyrolysis largely eliminates the oxygenated groups present in hydrothermal

carbonization. Therefore, HC has greater surface functionalization and chemical reactivity, while PIR is more graphitic and stable.

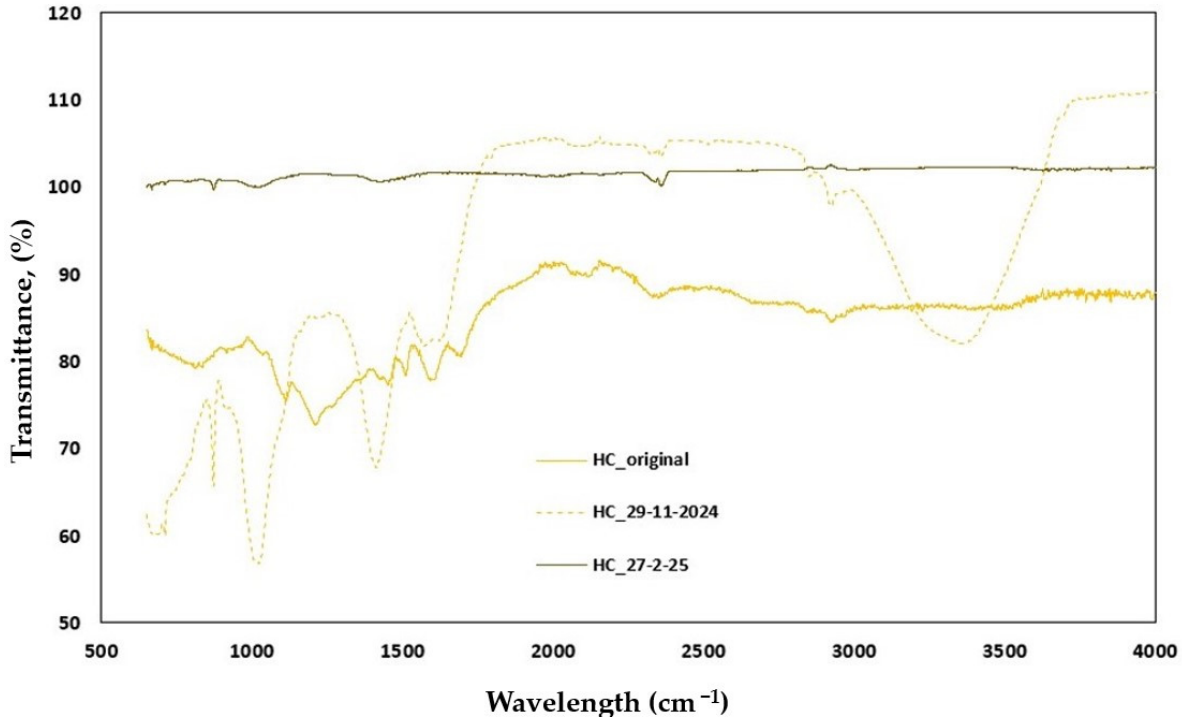


Figure 4. FTIR of HC during experimental time in soil.

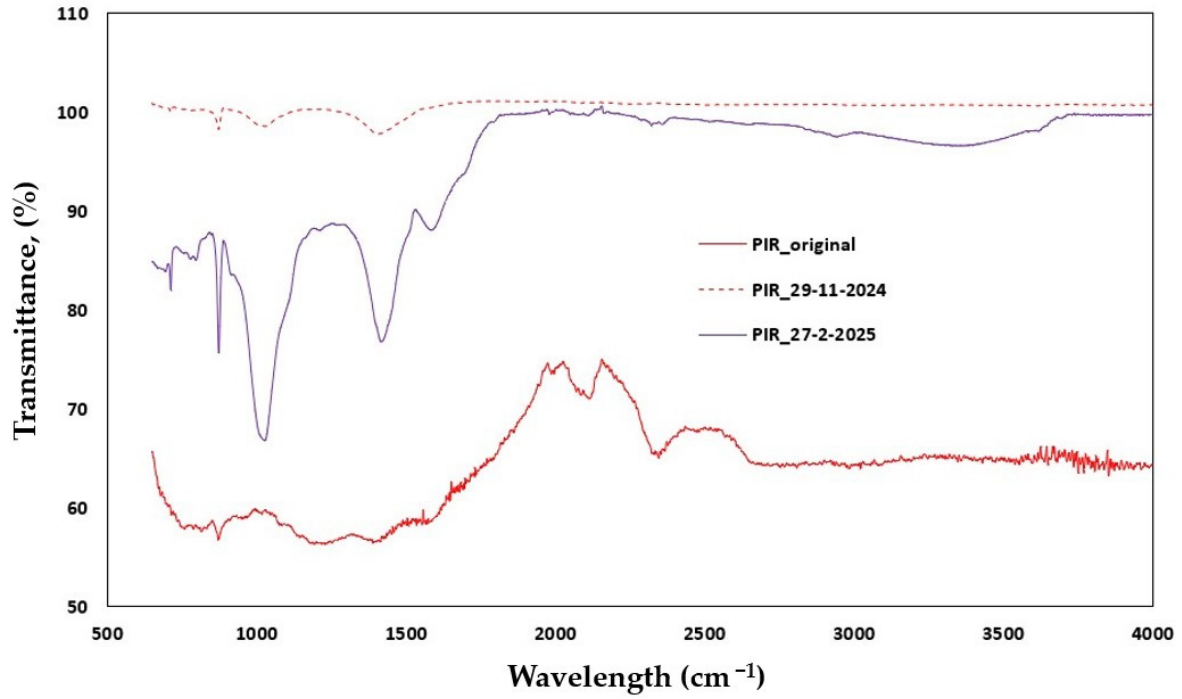


Figure 5. FTIR of PIR during experimental time in soil.

Secondly, the effect of iron (Fe) doping is analyzed (Figures 6 and 7). The Fe-doped samples show an additional band at 540–580 cm^{-1}, attributed to the formation of Fe-O bonds, confirming the presence of iron oxides on the surface. In addition, the following effects are observed:

1. The O-H and C=O bands do not decrease, indicating that the oxygenated functional groups remain after doping.
2. There is a slight decrease in the aliphatic C-H bands (2920 and 2850 cm^{-1}), possibly due to interactions between Fe and the carbon structure [43].
3. The aromatic C-H bands are less intense (~870, 810, and 750 cm^{-1}), suggesting a change in the structural organization of the carbon.

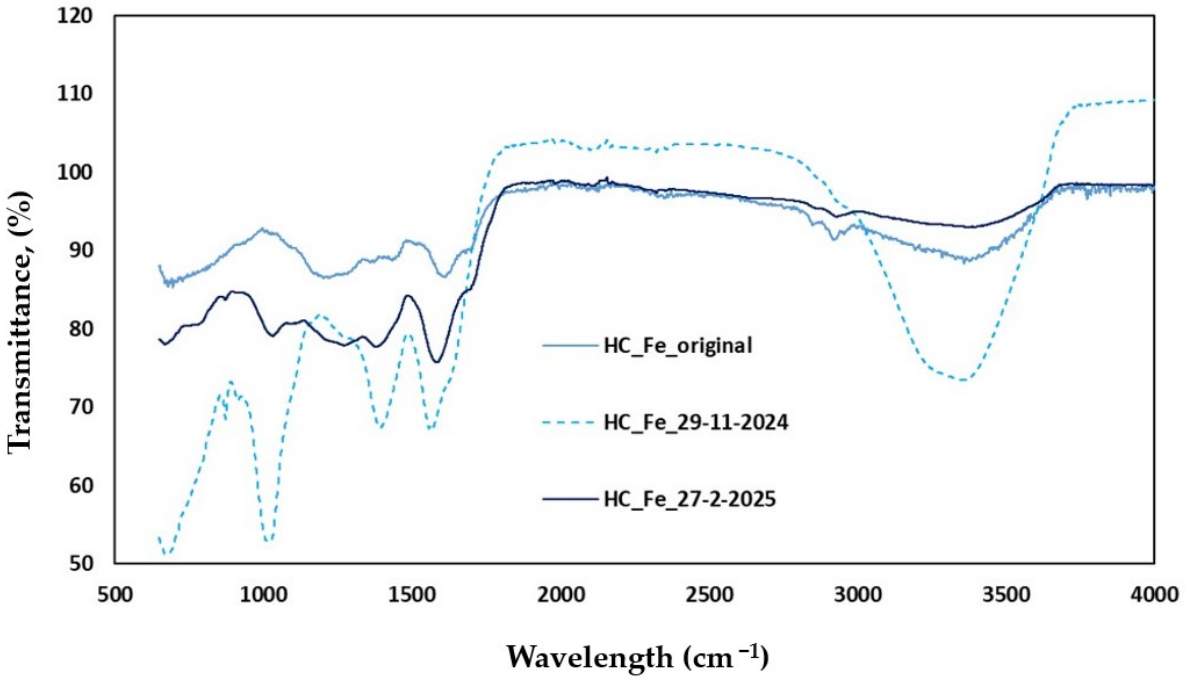


Figure 6. FTIR of HC_Fe during experimental time in soil.

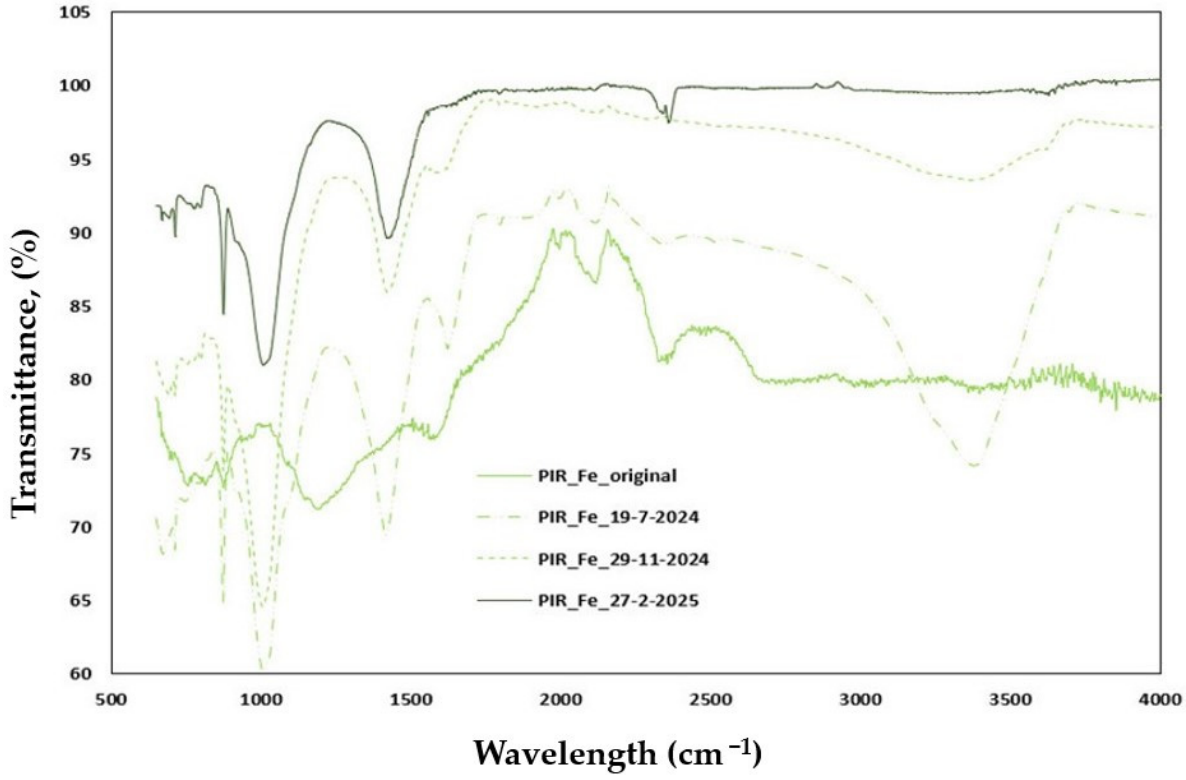


Figure 7. FTIR of PIR_Fe during experimental time in soil.

This confirms that Fe doping does not significantly alter surface functionalization but introduces magnetic properties due to the presence of iron oxides.

Table 5 summarizes the different peaks and functional groups found. Comparing the above with other studies, which also use vine residues versus other biomasses for soil amendment, yields different results. First, a study such as [26], focuses on the evaluation of a biochar with low aromatic and high aliphatic content, highlighting its lower structural stability but greater presence of oxygenated functional groups. Furthermore, this work directly compares two types of carbon obtained by different techniques: HTC and pyrolysis and analyzes the effect of iron doping on their structural properties.

Table 5. Key peaks and functional groups observed.

Functional Group	Peak (cm^{-1})	Observation
O-H (hydroxyls)	3200–3400	Higher intensity in HC; indicates presence of hydroxyl groups.
C=O (carbonyls: carboxylic acids and esters)	1700	Prominent in HC; attributed to carbonyl groups.
Aromatic C=C/COO^-	1600–1500	More pronounced in PIR; suggests more condensed aromatic/graphitic structure.
Aromatic specific signal	1580	Stronger in PIR; indicative of condensed aromatic structures.
C-O (alcohols and ethers)	1000–1200	More prominent in HC; reflects alcohol and ether functionalities.
Aliphatic C-H	2920; 2850	Slight decrease after Fe doping; possible interactions between Fe and carbon structure.
Aromatic C-H	~870; 810; 750	Reduced intensity after Fe doping; suggests changes in structural organization.

A key similarity between the two studies lies in the importance attributed to oxygenated functional groups (such as O-H, C=O, and C-O) [44], which are identified using Fourier transform infrared spectroscopy (FTIR). In both cases, the intensity of the bands corresponding to these groups is directly related to the surface functionalization of carbon. This could suggest that the presence of these groups improves the interaction of biochar with the soil, for which further research is needed; while the second study demonstrates that HC samples, obtained using HTC, exhibit greater intensity in these bands, indicating a surface richer in reactive groups compared to PIR samples.

The differences observed between the materials can be mainly attributed to experimental techniques. HTC tends to retain more oxygenated groups on the carbon surface, resulting in greater chemical reactivity. In contrast, pyrolysis, operating at higher temperatures and under drier conditions, favors the formation of condensed aromatic and graphitic structures, eliminating a large portion of the oxygenated groups. This technical difference explains why the PIR samples present a more intense signal in the aromatic bond region (1580 cm^{-1}) and lower intensity in the oxygenated functional group bands.

Another relevant aspect is the raw material used. The chemical composition of vineyard biomass, rich in lignin and phenolic compounds, can influence the formation of aromatic structures during pyrolysis, accentuating carbon graphitization. In contrast, if HTC is applied to the same raw material, the original functional groups are more likely to be preserved, which is reflected in the higher intensity of the O-H, C=O and C-O bands.

Finally, iron doping introduces an additional dimension as a novelty in this work. Although it does not significantly alter the presence of oxygenated groups, it does modify the structural organization of carbon, as indicated by the decrease in aliphatic and aromatic

bands. Furthermore, the appearance of bands attributable to Fe-O bonds confirms the incorporation of metal oxides, which could have implications for catalytic or magnetic applications, beyond the agronomic scope addressed in the first study [26]. Overall, comparing this study with previous ones, they agree that the surface functionalization of carbon is a determining factor in its properties and applications. The differences observed in the surface chemistry of grapevine-derived biochars are explained by the production techniques (HTC vs. PYR), the nature of the raw material (such as grapevine), and possible post-treatment chemical modifications (such as Fe doping). These variations confer distinct properties to the materials that could be relevant for different potential uses, ranging from exploratory soil studies to more advanced technological applications, the suitability of which will need to be evaluated through further specific research

4. Conclusions

This study provides a comparative physicochemical characterization of hydrochars (HCs) and pyrochars (PIRs) derived from vineyard stumps, including iron-enriched variants, and a preliminary assessment of plant tolerance based on chlorophyll index measurements. The results confirm that hydrothermal carbonization and pyrolysis generate carbonaceous materials with clearly distinct chemical structures. HCs retained a higher abundance of oxygen-containing functional groups, while PIRs exhibited a more condensed and aromatic carbon structure, consistent with their respective formation mechanisms. Iron incorporation was successfully achieved in both materials, as evidenced by FTIR analysis, introducing Fe–O bonds without eliminating surface oxygenated functionalities.

The vegetation experiment conducted in pots, designed as a preliminary screening to rule out obvious phytotoxic effects, showed that chlorophyll index values remained within the physiological ranges typically reported for grapevines across all treatments and sampling dates, and that the observed temporal variability was mainly due to seasonal and environmental factors. Although consistent trends related to the treatments cannot be established, these preliminary results highlight the potential of vineyard residues to be transformed into sustainable soil amendments that contribute to climate resilience, circular economy strategies, and improved soil quality.

In summary, the findings support the suitability of vineyard stumps as a feedstock for producing carbonaceous materials with differentiated properties through HTC and pyrolysis. The work establishes a solid material-level foundation and demonstrates initial plant compatibility under controlled conditions, which is a prerequisite for subsequent agronomic evaluation. Future research should involve replicated field trials with appropriate statistical designs, direct measurements of soil properties (e.g., pH, CEC, nutrient availability, moisture), and integrated plant physiological assessments to elucidate amendment–soil–plant interactions and medium- to long-term material stability. Additionally, iron-doped materials warrant further investigation for applications beyond agronomy, including nutrient management and environmental remediation.

Author Contributions: Conceptualization, S.R. and B.L.; methodology, J.M.D.-R., S.R. and T.S.; formal analysis, J.M.D.-R. and S.R.; investigation, J.M.D.-R., S.R., B.L. and T.S.; writing—original draft preparation, J.M.D.-R.; writing—review and editing, J.M.D.-R., B.L. and T.S.; visualization, J.M.D.-R., S.R. and B.L.; supervision, S.R.; project administration, S.R. and B.L.; funding acquisition, J.M.D.-R. and S.R. All authors have read and agreed to the published version of the manuscript.

Funding: This research was funded by JUNTA DE EXTREMADURA PhD Fellowship, grant number PD23085-5939110060220230002690, co-financed through the ESF+ fund. AGENCIA ESPAÑOLA DE INVESTIGACIÓN contributed with the financial help through project PID2024-157952OB-I00, funded under the ORGÁNICA program 18. GA.54.FA.

Data Availability Statement: The original contributions presented in the study are included in the article, further inquiries can be directed to the corresponding author.

Acknowledgments: The authors are thankful to SAIUEX (Servicios de Apoyo a la Investigación de la Universidad de Extremadura) have also contributed to this study by their support on analytical tests. The authors have reviewed and edited the output and take full responsibility for the content of this publication.

Conflicts of Interest: The authors declare no conflicts of interest.

Abbreviations

The following abbreviations are used in this manuscript:

VSs	Vineyard Stumps
PIR	Pyrochar
HC	Hydrochar
HTC	Hydrothermal carbonization
PYR	Pyrolysis
PIR_Fe	Pyrochars used in soil
HC_Fe	Hydrochar used in soil
HHV	Higher heating value
LHV	Lower heating value

References

1. Winter, S.; Bauer, T.; Strauss, P.; Kratschmer, S.; Paredes, D.; Popescu, D.; Landa, B.; Guzmán, G.; Gómez, J.A.; Guernion, M.; et al. Effects of vegetation management intensity on biodiversity and ecosystem services in vineyards: A meta-analysis. *J. Appl. Ecol.* **2018**, *55*, 2484–2495. [CrossRef]
2. Paiola, A.; Assandri, G.; Brambilla, M.; Zottini, M.; Pedrini, P.; Nascimbene, J. Exploring the potential of vineyards for biodiversity conservation and delivery of biodiversity-mediated ecosystem services: A global-scale systematic review. *Sci. Total Environ.* **2020**, *706*, 135839. [CrossRef]
3. Lazzari, M.; Piccarreta, M. Soil Erosion vs. Vineyard Productivity: The Case of the Aglianico del Vulture DOC and DOCG Areas (Southern Italy). *Sustainability* **2023**, *15*, 15700. [CrossRef]
4. Ferreira, C.S.S.; Seifollahi-Aghmiuni, S.; Destouni, G.; Ghajarnia, N.; Kalantari, Z. Soil degradation in the European Mediterranean region: Processes, status and consequences. *Sci. Total Environ.* **2022**, *805*, 150106. [CrossRef]
5. Cano, B.L.; Sánchez, M.A.; Rasero, J.M.D.; Suero, S.R.; Delgado, S.N. *Introduction to Hydrocarbonization: Principles and Applications*, 1st ed.; Springer: Cham, Switzerland, 2024; pp. 1–14.
6. Chen, W.H.; Biswas, P.P.; Zhang, C.; Kwon, E.E.; Chang, J.S. Achieving carbon credits through biomass torrefaction and hydrothermal carbonization: A review. *Renew. Sustain. Energy Rev.* **2025**, *208*, 115056. [CrossRef]
7. Wang, X.; Duo, J.; Jin, Z.; Yang, F.; Lai, T.; Collins, E. Effects of Hydrothermal Carbonization Conditions on the Characteristics of Hydrochar and Its Application as a Soil Amendment: A Review. *Agronomy* **2025**, *15*, 327. [CrossRef]
8. Bargmann, I.; Martens, R.; Rillig, M.C.; Kruse, A.; Kücke, M. Hydrochar amendment promotes microbial immobilization of mineral nitrogen. *J. Plant Nutr. Soil Sci.* **2014**, *177*, 59–67. [CrossRef]
9. Bargmann, I.; Rillig, M.C.; Kruse, A.; Greef, J.M.; Kücke, M. Effects of hydrochar application on the dynamics of soluble nitrogen in soils and on plant availability. *J. Plant Nutr. Soil Sci.* **2014**, *177*, 48–58. [CrossRef]
10. Xia, Y.; Luo, H.; Li, D.; Chen, Z.; Yang, S.; Liu, Z.; Yang, T.; Gai, C. Efficient immobilization of toxic heavy metals in multi-contaminated agricultural soils by amino-functionalized hydrochar: Performance, plant responses and immobilization mechanisms. *Environ. Pollut.* **2020**, *261*, 114217. [CrossRef] [PubMed]
11. Islam, M.A.; Limon, M.S.H.; Romić, M.; Islam, M.A. Hydrochar-based soil amendments for agriculture: A review of recent progress. *Arab. J. Geosci.* **2021**, *14*, 102. [CrossRef]
12. Sun, K.; Han, L.; Yang, Y.; Xia, X.; Yang, Z.; Wu, F.; Li, F.; Feng, Y.; Xing, B. Application of hydrochar altered soil microbial community composition and the molecular structure of native soil organic carbon in a paddy soil. *Environ. Sci. Technol.* **2020**, *54*, 2715–2725. [CrossRef]
13. Battipaglia, G.; Niccoli, F.; Kabala, J.P.; Marzaioli, R.; Di Santo, T.; Strumia, S.; Castaldi, S.; Rutigliano, F.A. Hydrochar application improves growth and intrinsic water use efficiency of *Populus alba*, especially during hot season. *Forests* **2023**, *14*, 658. [CrossRef]
14. Basso, D.; Weiss-Hortala, E.; Patuzzi, F.; Baratieri, M.; Fiori, L. In deep analysis on the behavior of grape marc constituents during hydrothermal carbonization. *Energies* **2018**, *11*, 1379. [CrossRef]

15. Pagés-Díaz, J.; Alvarado, A.O.C.; Montalvo, S.; Diaz-Robles, L.; Curio, C.H. Anaerobic bio-methane potential of the liquors from hydrothermal carbonization of different lignocellulose biomasses. *Renew. Energy* **2020**, *157*, 182–189. [CrossRef]
16. Zhang, B.; Heidari, M.; Regmi, B.; Salaudeen, S.; Arku, P.; Thimmannagari, M.; Dutta, A. Hydrothermal carbonization of fruit wastes: A promising technique for generating hydrochar. *Energies* **2018**, *11*, 2022. [CrossRef]
17. Hoffmann, V.; Jung, D.; Zimmermann, J.; Rodriguez Correa, C.; Elleuch, A.; Halouani, K.; Kruse, A. Conductive carbon materials from the hydrothermal carbonization of vineyard residues for the application in electrochemical double-layer capacitors (EDLCs) and direct carbon fuel cells (DCFCs). *Materials* **2019**, *12*, 1703. [CrossRef] [PubMed]
18. Lorero, I.; Vizcaíno, A.J.; Alguacil, F.J.; López, F.A. Activated carbon from winemaking waste: Thermoeconomic analysis for large-scale production. *Energies* **2020**, *13*, 6462. [CrossRef]
19. Baronti, S.; Magno, R.; Maienza, A.; Montagnoli, A.; Ungaro, F.; Vaccari, F. Long term effect of biochar on soil plant water relation and fine roots: Results after 10 years of vineyard experiment. *Sci. Total Environ.* **2022**, *838*, 158225. [CrossRef]
20. Giagnoni, L.; Maienza, A.; Baronti, S.; Vaccari, F.; Genesio, L.; Taiti, C.; Martellini, T.; Scodellini, R.; Cincinelli, A.; Costa, C.; et al. Long-term soil biological fertility, volatile organic compounds and chemical properties in a vineyard soil after biochar amendment. *Geoderma* **2019**, *337*, 122–131. [CrossRef]
21. Idbella, M.; Baronti, S.; Giagnoni, L.; Renella, G.; Becagli, M.; Cardelli, R.; Maienza, A.; Vaccari, F.P.; Bonanomi, G. Long-term effects of biochar on soil chemistry, biochemistry, and microbiota: Results from a 10-year field vineyard experiment. *Appl. Soil Ecol.* **2024**, *195*, 105217. [CrossRef]
22. Maienza, A.; Baronti, S.; Cincinelli, A.; Martellini, T.; Grisolia, A.; Miglietta, F.; Renella, G.; Stazi, S.; Vaccari, F.; Genesio, L. Biochar improves the fertility of a Mediterranean vineyard without toxic impact on the microbial community. *Agron. Sustain. Dev.* **2017**, *37*, 1–10. [CrossRef]
23. García-Jaramillo, M.; Meyer, K.; Phillips, C.; Acosta-Martínez, V.; Osborne, J.; Levin, A.; Trippe, K. Biochar addition to vineyard soils: Effects on soil functions, grape yield and wine quality. *Biochar* **2021**, *3*, 565–577. [CrossRef]
24. Aguirre, J.; González-Egido, S.; González-Lucas, M.; González-Pernas, F. Medium-term effects and economic analysis of biochar application in three Mediterranean crops. *Energies* **2023**, *16*, 4131. [CrossRef]
25. Schmidt, H.; Kammann, C.; Niggli, C.; Evangelou, M.; Mackie, K.; Abiven, S. Biochar and biochar-compost as soil amendments to a vineyard soil: Influences on plant growth, nutrient uptake, plant health and grape quality. *Agric. Ecosyst. Environ.* **2014**, *191*, 117–123. [CrossRef]
26. Uras, Ü.; Carrier, M.; Hardie, A.G.; Knoetze, J.H. Physico-chemical characterization of biochars from vacuum pyrolysis of South African agricultural wastes for application as soil amendments. *J. Anal. Appl. Pyrolysis* **2012**, *98*, 207–213. [CrossRef]
27. Marshall, J.; Muhlack, R.; Morton, B.J.; Dunnigan, L.; Chittleborough, D.; Kwong, C.W. Pyrolysis temperature effects on biochar–water interactions and application for improved water holding capacity in vineyard soils. *Soil Syst.* **2019**, *3*, 27. [CrossRef]
28. Videgain, M.; Marco, P.; Martí, C.; García-Ramos, F.J.; Manyà, J.J.; Jaizme-Vega, M.C. Evaluación de los efectos de la aplicación de biochar como enmienda orgánica en suelos agrícolas. In Proceedings of the Congreso Ibérico Agroingeniería 2019, Zaragoza, Spain, 3–6 September 2019; pp. 1–14. [CrossRef]
29. *ISO 3310-1*; Test Sieves—Technical Requirements and Testing—Part 1: Test Sieves of Metal Wire Cloth. ISO: Geneva, Switzerland, 2016.
30. Olivares-Marin, M.; Román, S.; Ledesma, B.; Álvarez, A. Optimizing Al and Fe Load during HTC of Water Hyacinth: Improvement of Induced HC Physicochemical Properties. *Catalysts* **2023**, *13*, 506. [CrossRef]
31. Gai, C.; Zhang, F.; Lang, Q.; Liu, T.; Peng, N.; Liu, Z. Facile One-Pot Synthesis of Iron Nanoparticles Immobilized into the Porous Hydrochar for Catalytic Decomposition of Phenol. *Appl. Catal. B Environ.* **2017**, *204*, 566–576. [CrossRef]
32. Uddling, J.; Gelang-Alfredsson, J.; Piikki, K.; Pleijel, H. Evaluating the relationship between leaf chlorophyll concentration and SPAD-502 chlorophyll meter readings. *Photosynth. Res.* **2007**, *91*, 37–46. [CrossRef]
33. Li, Q.; Zhang, Y.; Song, Y.; Yang, H.; Yang, L.; Bai, L.; Wei, D.; Wang, W.; Liang, Y.; Chen, H. Apple residues derived porous carbon nanosheets synthesized with $FeCl_3$ assisted hydrothermal carbonization for supercapacitors with high rate performance. *Carbon Lett.* **2023**, *33*, 549–560. [CrossRef]
34. MacDermid-Watts, K.; Adewakun, E.; Norouzi, O.; Deb, A.T.; Pradhan, R.; Dutta, A. Effects of $FeCl_3$ Catalytic Hydrothermal Carbonization on Chemical Activation of Corn Wet Distillers' Fiber. *ACS Omega* **2021**, *6*, 14875–14886. [CrossRef]
35. Liu, B.; Xing, Z.; Xue, Y.; Zhang, J.; Zhai, J. Effect of Pyrolysis Temperature on the Carbon Sequestration Capacity of Spent Mushroom Substrate Biochar in the Presence of Mineral Iron. *Molecules* **2024**, *29*, 5712. [CrossRef]
36. Ekpo, U.; Ross, A.B.; Camargo-Valero, M.A.; Fletcher, L.A. Influence of pH on hydrothermal treatment of swine manure: Impact on extraction of nitrogen and phosphorus in process water. *Bioresour. Technol.* **2016**, *214*, 637–644. [CrossRef]
37. Kruse, A.; Krupka, A.; Schwarzkopf, V.; Gamard, C.; Henningsen, T. Influence of Proteins on the Hydrothermal Gasification and Liquefaction of Biomass. 1. Comparison of Different Feedstocks. *Ind. Eng. Chem. Res.* **2005**, *44*, 3013–3020. [CrossRef]
38. Cerovic, Z.G.; Masdoumier, G.; Ghozlen, N.B.; Latouche, G. A new optical leaf-clip meter for simultaneous non-destructive assessment of leaf chlorophyll and epidermal flavonoids. *Physiol. Plant.* **2012**, *146*, 251–260. [CrossRef]

39. Canton, M.; Borghezan, M.; Silva, T.C.; Welter, J.F.; Villar, L.; Rosa, D.; Silva, A.L.; Pescador, R. Chlorophyll evaluation on leaves of 'Sauvignon Blanc' during vegetative growth in São Joaquim, Santa Catarina, Brazil. *Acta Hortic.* **2017**, *1188*, 15–20. [CrossRef]
40. Petrović, J.; Ercegović, M.; Simić, M.; Koprivica, M.; Dimitrijević, J.; Jovanović, A.; Janković Pantić, J. Hydrothermal Carbonization of Waste Biomass: A Review of Hydrochar Preparation and Environmental Application. *Processes* **2024**, *12*, 207. [CrossRef]
41. Lin, Q.; Yang, X.; Ma, W.; Zahoor, A.; Jin, F.; Chen, X.; Tai, L.; de Caprariis, B.; De Filippis, P.; Damizia, M. Hydrothermal carbonization of fish sludge: Effect of FeCl3 on the hydrochar properties and phosphorus and heavy metal transformation. *Environ. Technol. Innov.* **2025**, *40*, 104355. [CrossRef]
42. Zhang, X.; Wang, Y.; Li, J.; Chen, H. FTIR Analysis of Biomass and Its Application in Soil Studies. *IOP Conf. Ser. Earth Environ. Sci.* **2019**, *239*, 012035. [CrossRef]
43. Zhang, X.; Li, Y.; Wang, L.; Chen, H. Structural Characterization of Biomass Components Using FTIR Spectroscopy. *Int. J. Mol. Sci.* **2023**, *24*, 8936. [CrossRef]
44. Kocsis, T.; Buzás, N.; Farkas, I.; Kocsis, Z. Investigation of Biomass-Derived Materials Using FTIR and Thermal Analysis. *J. Agric. Environ. Sci.* **2025**, *8*, 870. [CrossRef]

Disclaimer/Publisher's Note: The statements, opinions and data contained in all publications are solely those of the individual author(s) and contributor(s) and not of MDPI and/or the editor(s). MDPI and/or the editor(s) disclaim responsibility for any injury to people or property resulting from any ideas, methods, instructions or products referred to in the content.